# A Simultaneous Hand-Eye Calibration Method for Hybrid Eye-in-Hand/Eye-to-Hand System

Shunan Ren*, Xu Yang*, Yongbo Song*, Hong Qiao*, Liao Wu†, Jing Xu‡, Ken Chen‡
*Institute of Automation, Chinese Academy of Sciences
Beijing, China, 100092, Email: renshunan@gmail.com.
†Australian Centre for Robotic Vision, School of Electrical Engineering and Computer Science,
Queensland University of Technology, Brisbane, Australia.
‡The Department of Mechanical and Engineering, Tsinghua University
Beijing, China, 100084.

***Abstract*—A hybrid system with both eye-in-hand and eye-to-hand configurations is often necessary for autonomous exploring equipment, such as ROVs. In order to localize objects accurately and grasp them rapidly, the relationships among the robot base, the end effector, the fixed cameras, and the cameras mounted on the end effector should be calibrated in advance. To achieve these goals, a fast calibration method is proposed in this paper, which could calibrate the hybrid camera system simultaneously. Then the feasibility and robustness of the proposed calibration method are verified by comparing it to the classical two-step method through simulations with different noise levels.**

***Index Terms*—Hand-eye calibration, Hybrid camera system, Hand-in-eye, Hand-to-eye, Simultaneous calibration method.**

## I. Introduction

When executing complex tasks under unstructured environments, like space and undersea exploration, mobile robots are usually equipped with multi sensors as perception sources.

In practice, the visual servo is still the most universal and robust control method. There are two most adopted camera configurations, which are, one or more cameras are attached to the end effector of the robot called eye-in-hand, and the other cameras are mounted on the base of the robot called eye-to-hand [1]. The eye-to-hand cameras have a panoramic view of the workspace, but a lower resolution. On the contrary, the eye-in-hand cameras can move close to the scene with the end effector's motion, thus clearer images of the object can be obtained while the sight is limited to the close range of the object. In order to make use of these advantages, several visual servo methods[2–5] have been studied recently to employ both eye-in-hand and eye-to-hand camera configurations.

Most visual servoing methods mentioned above are position based. The cameras are usually mounted on the end effector or the base of the robot to direct the action of the manipulator. To achieve accurate manipulation, the position of the object is first determined and the grasp action is then conducted. Intuitively, the critical point of accurate and rapid grasps is the coordination calibration among those cameras and the robot. Furthermore, it is necessary for the robot to change tools or cameras frequently to deal with varying task requirements. Thus an efficient and effective calibration method is urgently needed to be studied which timely and precisely evaluates the relationships among the robot end effector, the robot base and the eye-in-hand/eye-to-hand cameras.

When the camera is mounted on the end effector, the camera moves with the end effector synchronously. The hand-eye calibration problem was formulated as to solve a homogeneous matrix equation of the form **AX=XB** by Shiu and Ahmad [6] for the first time. In the equation above, **A** and **B** denote the homogeneous transformation matrices of the end effector and the eye-in-hand camera motions respectively, and **X** is the homogeneous transformation matrix which represents the relationship between the camera and the end effector. Soon Tsai proposed a classical two-step method[7]. Two or more relative spatial movements of the manipulator and camera with non-parallel screw axes are required to solve **X**. Since then many other methods [8–11]have been thoroughly investigated as well.

If an overall sight is needed, the camera is used to be fixed somewhere in the workspace of the manipulator. Then the target of calibration is to find the relationship between the robot frame and world frame attached to the fixed camera. This problem can be solved through at least two relative movements of the manipulator with respect to non-parallel screw axes as well. Furthermore, the mathematical expression was formulated as **AX=YB** [12, 13]. In the equation, **A** represents the transformation matrix from the robot base to the hand, **B** represents the calibrated exterior parameter of the camera to the target mounted on the robot hand, and **X** and **Y** represent the unknown relationships of tool-flange and robot-world respectively. Solutions to this problem have been also put forward in [14–16].

Moreover, some intuitive methods which calibrate hand-eye, robot-world, robot-robot relationships simultaneously have been developed[17–19]. By employing invariants during calibration process, probabilistic[18] and iterative[19] methods are used for solving the unknown transformation relationships and the results are shown to be satisfied. However, it is noted that the simultaneous calibration method which is appropriate for hybrid multi-eye system has not been studied before. With the prosperous development of service robots[20], industrial robots[3, 21] and remote-operated vehicles(ROVs)[22, 23], the hybrid visual servoing system is widely used for its more

accurate and robust control performance. Therefore, a rapid calibration method for this kind of system is worth being discussed.

Motivated by [19], we found the model of hybrid multi-eye system and then present the solution to this problem as well. In the following, a comparison between the proposed method and the two-step method is conducted through simulations with different levels of noises injected to the calibration data of cameras.

The reminder of this paper is structured as follows. Section II is dedicated to the illustration and formulation of the calibration problem. A mathematical iterative solution is then presented in Section III. Section IV demonstrates the simulation settings and analyzes the results with comparison to the two-step method. Finally, conclusions are provided in Section V.

## II. Problem Description

We assume two cameras are connected with the last joint link and fixed somewhere in the workspace of the manipulator respectively, as shown in Fig.1. Without loss of generality, two unknown constants are denoted as the homogeneous transformation matrices from the robot hand to the mounted camera(**X**) and from the robot base to the global camera(**Y**).

The state of the robot hand can be described as a homogeneous transformation $\mathbf{A}_i$ under the frame of the robot base in which $i$ means the $i$th movement. $\mathbf{A}_i$ is accessible with assumption that all kinematic parameters of the manipulator have been determined through calibration. Meanwhile, the descriptions of the target frame under eye-in-hand and eye-to-hand cameras are denoted as homogeneous transformations $\mathbf{B}_i$ and $\mathbf{C}_i$, respectively. Both variant matrices are measurable through the self calibrations of the cameras.

According to the invariant in the transformation loop, the relationship among the robot base and hand, eye-in-hand and eye-to-hand cameras can be expressed as

$$\mathbf{AXB} = \mathbf{YC} \tag{1}$$

with accessible matrices $\mathbf{A}_i$, $\mathbf{B}_i$, $\mathbf{C}_i$ and unknowns $\mathbf{X}_i$, $\mathbf{Y}_i$ to solve.

If one of the eye-in-hand/eye-to-hand cameras is replaced with a marker(such as a calibration panel), the problem can be solved by the classical two-step method. Assume that a marker is put on the robot hand, the **Y** can be treated and calculated as the **AX=YB** problem mentioned in [14, 16, 18]. Then the **X** can be solved with an additional marker in the workspace of the manipulator according to the **AX=XB** problem. Each step needs at least two relative motions of the manipulator and obtain 3 sets of data, which are ($\mathbf{A}_{1,2,3}$, $\mathbf{C}_{1,2,3}$) for **Y** and ($\mathbf{A}_{4,5,6}$, $\mathbf{B}_{4,5,6}$) for **X**.

In this paper, the proposed simultaneous method simplifies the data acquisition procedure in the two-step method with only one additional calibration panel. The entire calibration needs the manipulator and the calibration panel move just for once to determine the solution of the **AXB=YC** equation. Then 2 data sets ($\mathbf{A}_{1,2}$, $\mathbf{B}_{1,2}$, $\mathbf{C}_{1,2}$) are obtained with asynchronously

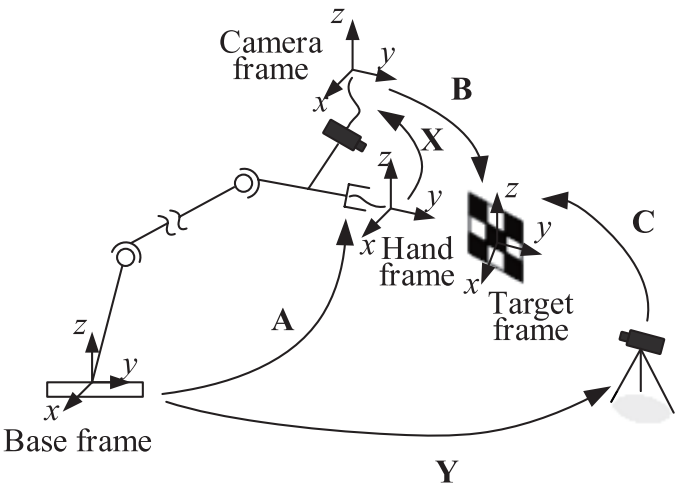


Fig. 1. The calibration problem can be formulated as **AXB=YC**, where **X** and **Y** are unknown relationships between the robot hand and eye-in-hand camera, the robot base and eye-to-hand camera, respectively.

movements of the manipulator and the calibration panel of which the screw axes are not parallel. The detailed iterative solution to this equation is described in Section III.

## III. An Iterative Solution to the Equation AXB=YC

We expand and rewrite **AXB=YC** as

$$\begin{bmatrix} \mathbf{R}_A & \mathbf{t}_\mathbf{A} \\ 0 & 1 \end{bmatrix} \begin{bmatrix} \mathbf{R}_X & \mathbf{t}_\mathbf{X} \\ 0 & 1 \end{bmatrix} \begin{bmatrix} \mathbf{R}_B & \mathbf{t}_\mathbf{B} \\ 0 & 1 \end{bmatrix} = \begin{bmatrix} \mathbf{R}_Y & \mathbf{t}_\mathbf{Y} \\ 0 & 1 \end{bmatrix} \begin{bmatrix} \mathbf{R}_C & \mathbf{t}_\mathbf{C} \\ 0 & 1 \end{bmatrix}. \tag{2}$$

Then the translational and rotational equations can be derived from the expanding homogeneous transformation matrix multiplication as:

$$\mathbf{R}_A\mathbf{R}_X\mathbf{R}_B = \mathbf{R}_Y\mathbf{R}_C, \tag{3}$$

$$\mathbf{R}_A\mathbf{R}_X\mathbf{t}_\mathbf{B} + \mathbf{R}_A\mathbf{t}_\mathbf{X} + \mathbf{t}_\mathbf{A} = \mathbf{R}_Y\mathbf{t}_\mathbf{C} + \mathbf{t}_\mathbf{Y}, \tag{4}$$

in which **R** stands for the 3×3 rotational component of the homogeneous transformation matrix, and **t** is the 3×1 translational component.

Specific to the equation **AXB=YC**, the solution can be found through transforming it into **AX=YB** problem. However, it is required in the classical method that at least one marker is mounted on the robot hand to calculate **Y**, which is a tedious procedure for the calibration of the hybrid-eye system. Thus we present a linear-approximation iterative method in this paper to solve $\mathbf{R}_X, \mathbf{R}_Y$ by using ($\mathbf{R}_{Ai}$, $\mathbf{R}_{Bi}$, $\mathbf{R}_{Ci}$) according to Eq.3. In the following, $\mathbf{t}_X, \mathbf{t}_Y$ can be directly calculated from Eq.4.

### A. Solution to the Unknown Rotational Components

According to [24], an arbitrary rotation matrix **R** which is an element of $SO(3)$ is the exponential function of its Lie algebra $[\boldsymbol{\omega}]^\wedge$ as

$$\mathbf{R} = e^{[\boldsymbol{\omega}]^\wedge} = \mathbf{I} + \frac{\sin(\|\boldsymbol{\omega}\|)}{\|\boldsymbol{\omega}\|}[\boldsymbol{\omega}]^\wedge + \frac{1-\cos(\|\boldsymbol{\omega}\|)}{\|\boldsymbol{\omega}\|^2}([\boldsymbol{\omega}]^\wedge)^2. \tag{5}$$

In Eq.5, $\omega = [\omega_1, \omega_2, \omega_3]^{\mathrm{T}}$ is a vector which contains both rotational axis and angle, while $\|\omega\|$ and $[\omega]^\wedge$ give the normal value and screw matrix of $\omega$ respectively.

Then the exponential map can be expanded into a sum of power series by using Taylor expansion, and it is obtained that:

$$\mathbf{R} = e^{[\omega]^\wedge} = \mathbf{I} + \sum_{n=1}^{\infty} \frac{([\omega]^\wedge)^n}{n!}. \tag{6}$$

The higher-order terms can be ignored with an assumption that $\mathbf{R}$ is in the neighborhood of the identity matrix $\mathbf{I}$, thus we have:

$$\mathbf{R} = e^{[\omega]^\wedge} = \mathbf{I} + [\omega]^\wedge. \tag{7}$$

This property can be used in solving $\mathbf{R}_X$, $\mathbf{R}_Y$ in our problem if we put back the rotation matrix into the neighborhood of $\mathbf{I}$ as follows:

$$\mathbf{R}_A(\mathbf{R}_X\mathbf{R}_{X0}^{-1})\mathbf{R}_{X0}\mathbf{R}_B = (\mathbf{R}_Y\mathbf{R}_{Y0}^{-1})\mathbf{R}_{Y0}\mathbf{R}_C, \tag{8}$$

in which $\mathbf{R}_i(i = X,Y)$ are the unknown exact values of the rotation matrices of $\mathbf{X}$ and $\mathbf{Y}$, whereas $\mathbf{R}_{i0}(i = X,Y)$ are corresponding guess values. Obviously, if the guess values are approximated enough to the true ones, Eq.7 can be substituted into Eq.8:

$$\mathbf{R}_A(\mathbf{I} + [\Delta\mathbf{r}_X]^\wedge)\mathbf{R}_{X0}\mathbf{R}_B = (\mathbf{I} + [\Delta\mathbf{r}_Y]^\wedge)\mathbf{R}_{Y0}\mathbf{R}_C, \tag{9}$$

in which $[\Delta\mathbf{r}_i]^\wedge$ are the associated Lie algebras of $\mathbf{R}_i\mathbf{R}_{i0}^{-1}(i = X,Y)$. Expanding Eq.9 and ignoring second-order infinitesimal terms, we have:

$$\mathbf{R}_A[\Delta\mathbf{r}_X]^\wedge\mathbf{R}_{X0}\mathbf{R}_B - [\Delta\mathbf{r}_Y]^\wedge\mathbf{R}_{Y0}\mathbf{R}_C = \mathbf{R}_{Y0}\mathbf{R}_C - \mathbf{R}_A\mathbf{R}_{X0}\mathbf{R}_B. \tag{10}$$

Due to the property of cross product operation and its corresponding screw matrix, the following relationship can be verified:

$$[\omega_a]^\wedge\omega_b = \omega_a \times \omega_b = -\omega_b \times \omega_a = -[\omega_b]^\wedge\omega_a. \tag{11}$$

Then, by using this property we can rearrange and expand Eq.10 by column and get the following equation:

$$\mathbf{G}\Delta\mathbf{r} = \mathbf{u}, \tag{12}$$

in which

$$\mathbf{G} = \begin{bmatrix} -\mathbf{R}_A[(\mathbf{R}_{X0}\mathbf{R}_B)_1]^\wedge & [(\mathbf{R}_{Y0}\mathbf{R}_C)_1]^\wedge \\ -\mathbf{R}_A[(\mathbf{R}_{X0}\mathbf{R}_B)_2]^\wedge & [(\mathbf{R}_{Y0}\mathbf{R}_C)_2]^\wedge \\ -\mathbf{R}_A[(\mathbf{R}_{X0}\mathbf{R}_B)_3]^\wedge & [(\mathbf{R}_{Y0}\mathbf{R}_C)_3]^\wedge \end{bmatrix}_{9\times 6}, \tag{13}$$

$$\Delta\mathbf{r} = [\ \Delta\mathbf{r}_X^T \quad \Delta\mathbf{r}_Y^T\ ]_{6\times 1}^T, \tag{14}$$

$$\mathbf{u} = \begin{bmatrix} (\mathbf{R}_{Y0}\mathbf{R}_C - \mathbf{R}_A\mathbf{R}_{X0}\mathbf{R}_B)_1 \\ (\mathbf{R}_{Y0}\mathbf{R}_C - \mathbf{R}_A\mathbf{R}_{X0}\mathbf{R}_B)_2 \\ (\mathbf{R}_{Y0}\mathbf{R}_C - \mathbf{R}_A\mathbf{R}_{X0}\mathbf{R}_B)_3 \end{bmatrix}_{9\times 1}. \tag{15}$$

and $(-)_i(i = 1,2,3)$ means the $i$th column vector in the bracket.

Indeed, once the manipulator moves or the pose of the calibration panel is changed, an equation in the form of Eq.12 can be obtained for every measurement. Concatenating these equations together, hence we have:

$$\tilde{\mathbf{G}}\Delta\mathbf{r} = \tilde{\mathbf{u}} \tag{16}$$

in which

$$\tilde{\mathbf{G}} = [\ \mathbf{G}_1^T \quad \mathbf{G}_2^T \quad \cdots \quad \mathbf{G}_n^T\ ]_{9n\times 9}^T \tag{17}$$

$$\tilde{\mathbf{u}} = [\ \mathbf{u}_1^T \quad \mathbf{u}_2^T \quad \cdots \quad \mathbf{u}_n^T\ ]_{9n\times 1}^T \tag{18}$$

and $n$ represents $n$ sets of measurement data.

Associate with the solution of non-homogeneous linear equations, it is naturally suggested that the least-square method can be employed to solve $\Delta\mathbf{r}$.

$$\Delta\mathbf{r} = (\tilde{\mathbf{G}}^T\tilde{\mathbf{G}})^{-1}\tilde{\mathbf{G}}^T\tilde{\mathbf{u}} \tag{19}$$

Extracting $\Delta\mathbf{r}_i(i = X,Y)$ with respect to $\mathbf{X}$, $\mathbf{Y}$ from $\Delta\mathbf{r}$, the initial guessed rotation matrix can be updated with

$$\mathbf{R}_{i0}^{(n+1)} = e^{[\Delta\mathbf{r}_i]^\wedge}\mathbf{R}_{i0}^{(n)}(i = X,Y). \tag{20}$$

The iterative procedure runs towards at least a local optimal solution until a preset threshold is reached. To guarantee a global optimum, the initial rotation matrices should be good enough. In fact, the initial guess values are also critical to ensure the effectiveness of this algorithm according to Eq.8 and Eq.9. Fortunately, the poses of both cameras can be approximately evaluated considering their mechanical mounting dimensions.

### *B. Solution to the Unknown Translational Components*

Compared with the rotational components, the solution to the translational components is effortless. Rearrange Eq.4 and we have:

$$\mathbf{H}\mathbf{t} = \mathbf{v} \tag{21}$$

in which

$$\mathbf{H} = [\ \mathbf{R}_A \quad -\mathbf{I}\ ]_{3\times 6}, \tag{22}$$

$$\mathbf{t} = [\ \mathbf{t}_X^T \quad \mathbf{t}_Y^T\ ]_{6\times 1}^T, \tag{23}$$

$$\mathbf{v} = -\mathbf{t}_A - \mathbf{R}_A\mathbf{R}_X\mathbf{t}_B + \mathbf{R}_Y\mathbf{t}_C. \tag{24}$$

As with Eq.16 for solving rotational matrices, we can use $n$ sets of measured data and stacking them up into

$$\tilde{\mathbf{H}}\mathbf{t} = \tilde{\mathbf{v}} \tag{25}$$

in which

$$\tilde{\mathbf{H}} = [\ \mathbf{H}_1^T \quad \mathbf{H}_2^T \quad \cdots \quad \mathbf{H}_n^T\ ]_{3n\times 6}^T, \tag{26}$$

$$\tilde{\mathbf{v}} = [\ \mathbf{v}_1^T \quad \mathbf{v}_2^T \quad \cdots \quad \mathbf{v}_n^T\ ]_{3n\times 1}^T. \tag{27}$$

Therefore, we can solve $\mathbf{t}$ by

$$\mathbf{t} = (\tilde{\mathbf{H}}^T\tilde{\mathbf{H}})^{-1}\tilde{\mathbf{H}}^T\tilde{\mathbf{v}}. \tag{28}$$

## IV. Simulations

### A. Simulation Environment and Results

To verify the effectiveness and robustness of the algorithm proposed in this paper and compare it with previous methods, several simulations are performed with the amount and noise level of the measured data as variables. Without loss of generality, a UR5 robot which has 6 degrees of freedom(DOFs) is employed in the simulation environment. The kinematic parameters of UR5 are referred to [25].

Which is different from [19], the movement of the manipulator alone does not change the measured data of $\mathbf{C}$. And it is impossible to acquire the unique solution when $\mathbf{F}$ is singular due to the same $\mathbf{R_C}$. Hence the data set can be acquired as following schemes. Once the pose of the calibration panel is changed, ten sets of measured data are organized into a data group with the robot hand moves for ten times. Thus the total amount of the data sets is $10n$ suppose the calibration panel moves for $n$ times.

The true and initial values of $\mathbf{X}$ and $\mathbf{Y}$ are preset for all simulations as shown in the Table.I. Furthermore, composite noises are added into the measured data of cameras to simulate the real environment approximately which are described in Table.II. The noises are subject to Gaussian distributions and three levels are preset. For rotational components, the noises are injected into the original Euler angles $\theta_{lj}(l = B,C; j = \alpha,\beta,\gamma)$ and each of the expectations $\mu_{lj}$ of the noise distributions is set as the corresponding true value. Meanwhile, the translational noises are added to the every component $t_{lk}(k = x,y,z)$ and the expectations $\tau_{lk}$ are the true values as well.

The calculation errors can be evaluated through the definitions as follows:

$$\varepsilon_r = \theta(\mathbf{R}_{i,\text{cal}}\mathbf{R}_{i,\text{true}}^{-1}) \tag{29}$$

and

$$\varepsilon_t = \left\|\mathbf{t}_{i,\text{cal}} - \mathbf{t}_{i,\text{true}}\right\|, \tag{30}$$

in which $\varepsilon_r$ and $\varepsilon_t$ stands for the rotational and translational errors respectively. $\theta(-)$ is the rotational angle of the matrix it works on, while $(-)_{i,\text{cal}}$ and $(-)_{i,\text{true}}$ represent the calculation results and true values of the rotational matrices $\mathbf{R}_i$ and translational vectors $\mathbf{t}_i$ with $i$ meaning the unknown transformation matrices $\mathbf{X}$, $\mathbf{Y}$.

The simulation results are divided into the rotational and translational errors and shown in Fig.2. In all figures, the solid red lines represent the results of the proposed method while the dash blue lines are that of the classical two-step method.

### B. Analysis and Discussion

It is clearly shown that most results of both methods keep stable convergence while the rest oscillate around the neighborhoods of the true values due to the high-level noises. Meanwhile, the calibration accuracy decreases for both methods with the noises getting strengthened. Definitely, the sensitivity to the noises of the simultaneous method are lower compared with the two-step method which shows its superiority on the robustness and accuracy. Thus the simultaneous method performs significant improvement in the terms of rotational and translational errors while some higher translational errors are temporarily obtained during early calculation.

In most cases for the simultaneous method, errors decreases sharply with the data sets involved in the calculation increasing. A rapid convergence can be obtained with 50 data sets, namely only 5 pose changes of the calibration panel are needed to be made. By contrast, much more measured data sets are required for the two-step method to gain the same level of accuracy with considering that two calibration panels have to be handled sequently which is tedious and time consuming for the practical operation.

## V. Conclusion

In this paper, a hybrid calibration problem for eye-in-hand/eye-to-hand cameras is proposed and formulated as a matrix equation **AXB=YC**. Inspired by the former research, we put forward a linear approximation iterative solution to this problem, which is shown to be efficient and robust to converge to the true values of the unknowns $\mathbf{X}$ and $\mathbf{Y}$ simultaneously in the simulations. The comparison with the classical two-step method highlights the overwhelming performance of the proposed method in the aspects of accuracy, efficiency and robustness.

In the future work, physical experiments are to be carried out to verify the effectiveness and practicability of the algorithm for practical use, for example, deep sea or space exploration. And the pose changes of the calibration panel and the manipulator will be also studied to enhance the operability.

## Acknowledgment

This work is supported partly by the National Key Research and Development Plan of China (Grant 2016YFC0300801), partly by the National Natural Science Foundation (NSFC) of China (Grants 61503383, 61633009 61627808, 91648205), and partly by the Strategic Priority Research Program of the Chinese Academy of Sciences (Grant XDB02080003).

## References

[1] Seth Hutchinson, Gregory D Hager, and Peter I Corke. A tutorial on visual servo control. *IEEE transactions on robotics and automation*, 12(5):651–670, 1996.

[2] Xinwu Liang, Hesheng Wang, Yun-Hui Liu, Weidong Chen, and Jie Zhao. A unified design method for adaptive visual tracking control of robots with eye-in-hand/fixed camera configuration. *Automatica*, 59:97–105, 2015.

[3] Ren C Luo, Shih-Che Chou, Xin-Yi Yang, and Norman Peng. Hybrid eye-to-hand and eye-in-hand visual servo system for parallel robot conveyor object tracking and

TABLE I
PRESETS OF **X** AND **Y**

| Items | True Value | Initial Value |
|---|---|---|
| **X** | $\begin{bmatrix} -1 & 0 & 0 & 0 \\ 0 & -1 & 0 & 20 \\ 0 & 0 & 1 & -50 \\ 0 & 0 & 0 & 1 \end{bmatrix}$ | $\begin{bmatrix} -0.9525 & 0.1851 & -0.2419 & 3 \\ -0.1081 & -0.9478 & -0.2998 & 22 \\ -0.2848 & -0.2594 & 0.9228 & -48 \\ 0 & 0 & 0 & 1 \end{bmatrix}$ |
| **Y** | $\begin{bmatrix} 0 & 0 & -1 & -100 \\ 1 & 0 & 0 & -300 \\ 0 & -1 & 0 & 100 \\ 0 & 0 & 0 & 1 \end{bmatrix}$ | $\begin{bmatrix} -0.4044 & -0.0298 & -0.9141 & -105 \\ 0.9018 & 0.1536 & -0.4040 & -294 \\ 0.1524 & -0.9877 & -0.0352 & 96 \\ 0 & 0 & 0 & 1 \end{bmatrix}$ |

TABLE II
THREE LEVELS OF GAUSSIAN NOISES ARE ADDED INTO THE MEASURED DATA.

| | High Level of Noises | Medium Level of Noises | Low Level of Noises |
|---|---|---|---|
| Rotational Component(degree) | $\theta_{lj} \sim N(\mu_{lj}, 0.2)$ | $\theta_{lj} \sim N(\mu_{lj}, 0.1)$ | $\theta_{lj} \sim N(\mu_{lj}, 0.01)$ |
| Translational Component(mm) | $t_{lk} \sim N(\tau_{lk}, 2)$ | $t_{lk} \sim N(\tau_{lk}, 1)$ | $t_{lk} \sim N(\tau_{lk}, 0.1)$ |


fetching. In *Industrial Electronics Society, IECON 2014-40th Annual Conference of the IEEE*, pages 2558–2563. IEEE, 2014.

[4] Abdul Muis and Kouhei Ohnishi. Eye-to-hand approach on eye-in-hand configuration within real-time visual servoing. *IEEE/ASME transactions on Mechatronics*, 10(4):404–410, 2005.

[5] Hong Qiao, Peng Zhang, Bo Zhang, and Suiwu Zheng. Learning an intrinsic-variable preserving manifold for dynamic visual tracking. *IEEE Transactions on Systems, Man, and Cybernetics, Part B (Cybernetics)*, 40(3):868–880, 2010.

[6] Yiu Cheung Shiu and Shaheen Ahmad. Calibration of wrist-mounted robotic sensors by solving homogeneous transform equations of the form ax= xb. *ieee Transactions on Robotics and Automation*, 5(1):16–29, 1989.

[7] Roger Y Tsai and Reimar K Lenz. A new technique for fully autonomous and efficient 3d robotics hand/eye calibration. *IEEE Transactions on robotics and automation*, 5(3):345–358, 1989.

[8] Frank C Park and Bryan J Martin. Robot sensor calibration: solving ax= xb on the euclidean group. *IEEE Transactions on Robotics and Automation*, 10(5):717–721, 1994.

[9] Hanqi Zhuang, Kuanchih Wang, and Zvi S Roth. Simultaneous calibration of a robot and a hand-mounted camera. *IEEE Transactions on Robotics and Automation*, 11(5):649–660, 1995.

[10] Sang De Ma. A self-calibration technique for active vision systems. *IEEE Transactions on Robotics and Automation*, 12(1):114–120, 1996.

[11] Irene Fassi and Giovanni Legnani. Hand to sensor calibration: A geometrical interpretation of the matrix equation ax= xb. *Journal of Field Robotics*, 22(9):497–506, 2005.

[12] Hanqi Zhuang, Zvi S Roth, and Raghavan Sudhakar. Simultaneous robot/world and tool/flange calibration by solving homogeneous transformation equations of the form ax= yb. *IEEE Transactions on Robotics and Automation*, 10(4):549–554, 1994.

[13] Fadi Dornaika and Radu Horaud. Simultaneous robot-world and hand-eye calibration. *IEEE transactions on Robotics and Automation*, 14(4):617–622, 1998.

[14] Robert L Hirsh, Guilherme N DeSouza, and Avinash C Kak. An iterative approach to the hand-eye and base-world calibration problem. In *Robotics and Automation, 2001. Proceedings 2001 ICRA. IEEE International Conference on*, volume 3, pages 2171–2176. IEEE, 2001.

[15] Floris Ernst, Lars Richter, Lars Matthäus, Volker Martens, Ralf Bruder, Alexander Schlaefer, and Achim Schweikard. Non-orthogonal tool/flange and robot/world calibration. *The International Journal of Medical Robotics and Computer Assisted Surgery*, 8(4):407–420, 2012.

[16] Jan Heller, Didier Henrion, and Tomas Pajdla. Hand-eye and robot-world calibration by global polynomial optimization. In *Robotics and Automation (ICRA), 2014 IEEE International Conference on*, pages 3157–3164. IEEE, 2014.

[17] Aiguo Li, Lin Wang, and Defeng Wu. Simultaneous robot-world and hand-eye calibration using dual-quaternions and kronecker product. *International Journal of Physical Sciences*, 5(10):1530–1536, 2010.

[18] Haiyuan Li, Qianli Ma, Tianmiao Wang, and Grego-

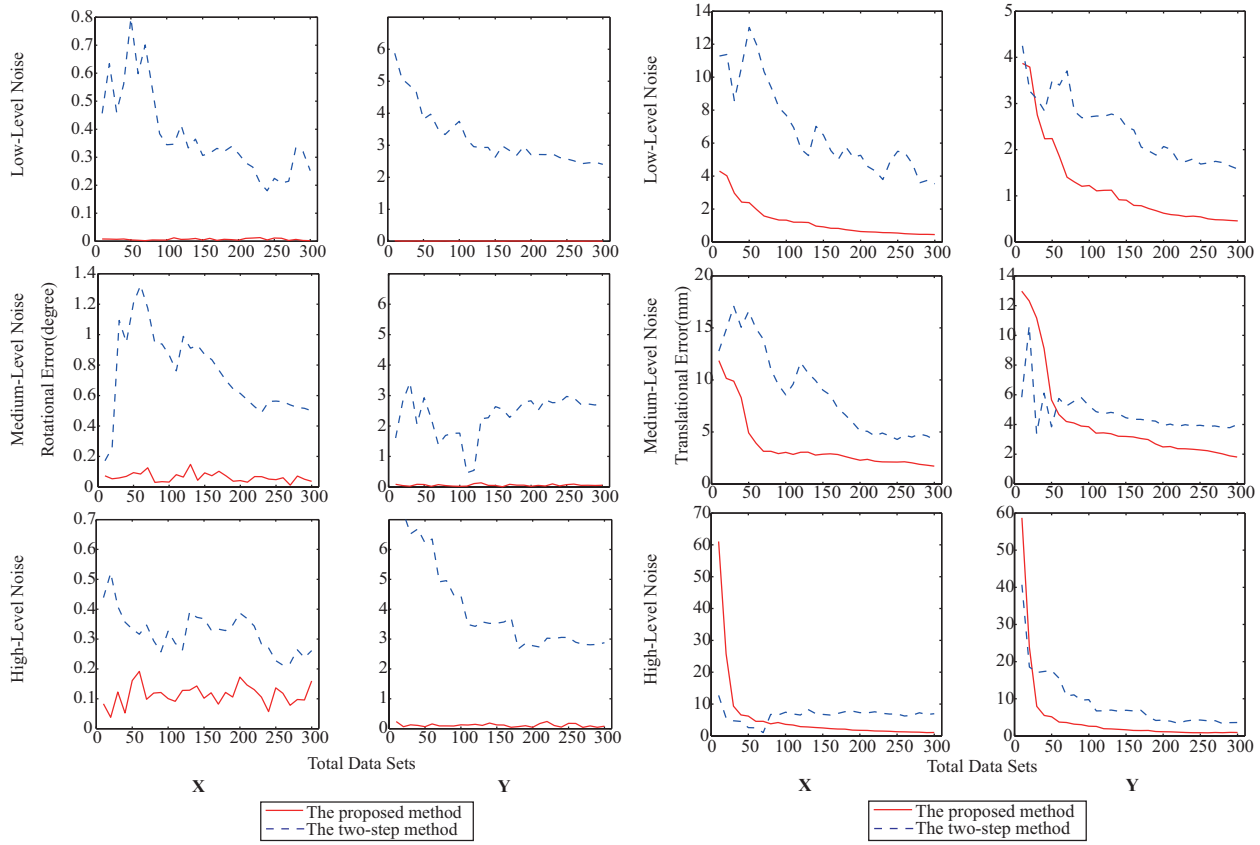


(a) The Rotational Errors

(b) The Translational Errors

Fig. 2. The calibration errors(including rotational and translational errors) of unknown relationship **X** and **Y** are shown with different noise levels and contained data sets for two methods.


ry S Chirikjian. Simultaneous hand-eye and robot-world calibration by solving the **AX=YB** problem without correspondence. *IEEE Robotics and Automation Letters*, 1(1):145–152, 2016.

[19] Liao Wu, Jiaole Wang, Lin Qi, Keyu Wu, Hongliang Ren, and Max Q-H Meng. Simultaneous hand-eye, tool-flange, and robot-robot calibration for comanipulation by solving the **AXB=YCZ** problem. *IEEE Transactions on Robotics*, 32(2):413–428, 2016.

[20] Claire Dune, Eric Marchand, and Christophe Leroux. One click focus with eye-in-hand/eye-to-hand cooperation. In *Robotics and Automation, 2007 IEEE International Conference on*, pages 2471–2476. IEEE, 2007.

[21] Vincenzo Lippiello, Bruno Siciliano, and Luigi Villani. Position-based visual servoing in industrial multirobot cells using a hybrid camera configuration. *IEEE Transactions on Robotics*, 23(1):73–86, 2007.

[22] José Javier Fernández, Mario Prats, Pedro J Sanz, Juan Carlos García, Raul Marin, Mike Robinson, David Ribas, and Pere Ridao. Grasping for the seabed: Developing a new underwater robot arm for shallow-water intervention. *IEEE Robotics & Automation Magazine*, 20(4):121–130, 2013.

[23] Ying Wang, Guan-lu Zhang, Haoxiang Lang, Bashan Zuo, and Clarence W De Silva. A modified image-based visual servo controller with hybrid camera configuration for robust robotic grasping. *Robotics and Autonomous Systems*, 62(10):1398–1407, 2014.

[24] Jon M Selig. *Geometric fundamentals of robotics*. Springer Science & Business Media, 2004.

[25] Signe Moe, Gianluca Antonelli, Kristin Y Pettersen, and Johannes Schrimpf. Experimental results for set-based control within the singularity-robust multiple task-priority inverse kinematics framework. In *Robotics and Biomimetics (ROBIO), 2015 IEEE International Conference on*, pages 1233–1239. IEEE, 2015.